Simulations of Axial Bunch Compression in Heavy Ion Rings for Plasma Physics Applications at GSI*

S.M. Lund[a], O. Boine-Frankenheim[b], G. Franchetti[b], I. Hofmann[b], P. Spiller[b]
[a] Lawrence Livermore National Laboratory (LLNL), Livermore, CA 94550, USA
[b] Gesellschaft für Schwerionenforschung (GSI), D-64220 Darmstadt, Germany

Abstract

Simulations of axial bunch compression in heavy-ion rings have been carried out as part of a feasibility study for generating intense beams in a facility at GSI. The compression is implemented by a fast rotation of the longitudinal ($\|$) phase space and results in greatly increased transverse ($\perp$) space-charge strength while the bunch is compressed in a dispersive ring from an initial prebunch with a $\|$ momentum spread of $\Delta p/p \sim 10^{-4}$ (full half-width) to a final spread of $\Delta p/p \simeq 1\%$ at the final focus optic. The need to maintain beam quality during the compression results in numerous issues that are explored with PIC simulations.

1 INTRODUCTION

Plasma physics experiments at GSI are being designed to produce dense, large-volume plasmas with heavy-ion beams for use in general scientific research and in exploring target issues in Heavy-Ion Fusion. These applications require high beam intensity on target with small focal spots and short pulse durations. Overall system configurations under consideration to achieve the needed parameters are discussed in a related paper[1]. Here, we examine the final $\|$ bunching needed to achieve such high intensities. Economic considerations dictate that the bunching is best carried out in a ring using a fast rotation of the $\|$ phase-space. Parameters for 18 T-m and 100 T-m compressor rings (CR-18 and CR-100), which represent a range of bunching options, are summarized in Table 1. Bunching rings with similar compression physics are also under development at RIKEN and ITEP. The bunching waveforms needed for these options are consistent with conventional, low-frequency magnetic alloy RF "cavities" or new, high repetition rate induction cells developed at LLNL[2]. For cavity/cell superpositions that approximate ideal, linear bunching waveforms, little difference is expected in the physics of bunching implemented by RF and induction technologies[2]. Thus, here we assume linear RF bunching.

2 SIMULATIONS

A hierarchy of simulations with increasing model detail has been developed to investigate the compression of a bunch of N particles of rest mass m and charge q moving in a ring of radius R about a coasting, synchronous particle with $\|$ kinetic energy $\mathcal{E}_s = (\gamma_s - 1)mc^2$. Here, c is the speed of light in vacuo, and $\gamma_s = 1/\sqrt{1-\beta_s^2}$, where $\beta_s c$ is the $\|$ velocity of the synchronous particle.

2.1 Envelope Simulations

Parametric changes associated with ideal bunch compressions are first analyzed with a simple envelope model. In this model, continuous bending (ring radius R) and $\perp$ and $\|$ focusing are assumed along with linear particle equations of motion consistent with a $\|$ Neuffer distribution and a $\perp$ matched, KV distribution. The line-charge density within the bunch is parabolic with $\lambda \propto 1 - (\delta z/r_z)^2$, where δz is the $\|$ coordinate relative to the synchronous particle and the $\|$ bunch radius r_z evolves according to the envelope equation

$$r_z'' + k_{0s}^2 r_z - \frac{K_\|}{r_z^2} - \frac{\epsilon_\|^2}{r_z^3} = 0. \qquad (1)$$

Here, primes denote d/ds, where s is $\|$ propagation distance of the bunch, k_{0s} is the synchrotron wavenumber in the linear RF approximation, $K_\|$ is the space-charge perveance (dimension length), and $\epsilon_\| = const$ is the rms emittance. More explicitly, $k_{0s}^2 = qVh|\eta|/(2\pi R^2 \gamma_s \beta_s^2 mc^2)$ for an RF cavity operating on harmonic h (h = number of bunches) with a maximum voltage gain per turn of V, $K_\| = 3\bar{g}q^2 N|\eta|/(2\gamma_s^3\beta_s^2 mc^2)$ where $\bar{g}$ is an average of the geometric factor $g = 1/2 + 2\ln(r_p/r_b)$ (r_p and r_b are the $\perp$ pipe-radius and bunch radius of the matched KV beam; $\bar{g}$ includes weak $\perp$ / $\|$ coupling[2]), and $\epsilon_\| = |\eta| r_z \Delta p/p = const$ where $\Delta p/p$ is the half-width of the $\|$ distribution in the fractional particle off-momentum $\delta p/p$. Here, $\eta = 1/\gamma_t^2 - 1/\gamma_s^2 < 0$ is the "slip factor" with transition gamma $\gamma_t \simeq Q_{0x}$ [Q_{0x} and Q_{0y} are the horizontal (x-plane) and vertical (y-plane) undepressed tunes].

The envelope equation (1) is integrated from an initial ($s = 0$) prebunch to estimate parametric changes due to a compression induced by a sudden increase in RF voltage V. Results are shown in Fig. 1 as a function of ring laps $[s/(2\pi R)]$ for CR-18 parameters, a single bunch ($h = 1$), and a half-ring prebunch ($r_z = \pi R/2$). Results of this compression and an analogous one for CR-100 are summarized in Table 1. The compression corresponds to a 90°

Table 1: Ring parameters and envelope model results.

Parameter	CR-18	CR-100
Ion	U_{238}^{+28}	U_{238}^{+4}
Ring Radius, R [m]	34.49	157
Ring Lattice Periods, M	12	60
Pipe Radius, r_p [cm]	10	10
$\perp$ Tunes, Q_{0x}, Q_{0y}	4.2, 3.4	10.8, 9.7
Particle K.E., $\mathcal{E}_s$ [MeV/u]	200	127
Particle Number, N	2×10^{11}	8.5×10^{12}
$\perp$ Emittances, $\epsilon_x = \epsilon_y$ [mm-mr]	10	20
$\|$ Emittance, ϵ_z [m-mr]	16.8	20.7
Envelope Model Results		
RF Voltage ($h = 1$), V [kV]	560	3000
Laps for Compression	59.475	49.412
Prebunch, 1/2 Ring, Mid-Pulse		
Tune Depression, σ/σ_0	0.978,	0.994,
Momentum Spread $\Delta p/p$	5×10^{-4}	1.1×10^{-4}
Full Compression, Mid-Pulse		
Pulse Duration τ_p [ns]	32	39
Tune Depression, σ/σ_0	0.652	0.592
Tune shift, ΔQ	−1.32	−4.18
Momentum Spread $\Delta p/p$	0.01	0.01

* Research performed by LLNL, US DOE contract W-7405-ENG-48.

rotation of the initial phase-space ellipse and takes place in 59.475 laps [$59.475 > (1/4)/(Rk_{s0}) = 59.147$ due to space-charge]. As the full-width pulse duration $\tau_p = 2r_z/(\beta_s c)$ decreases, the $\perp$ space-charge becomes stronger as measured by the decrease in σ/σ_0 (σ and σ_0 are the phase advance per lattice period of $\perp$ particle oscillations with and without space-charge) or the increase in tune shift $\Delta Q = (1-\sigma/\sigma_0)k_{\beta 0}R$, where $k_{\beta 0} = (Q_{x0}+Q_{y0})/(2R)$. This increase in space-charge strength occurs rapidly over the final phase of the rotation and is accompanied by a large increase in the momentum-spread width of the distribution, $\Delta p/p$. This spread contains a coherent component, $(\Delta p/p)|_c = (r'_z/|\eta|)(\delta z/r_z)$, that nulls at full compression (upright phase-space ellipse with $r'_z = 0$) and an incoherent component, $(\Delta p/p)|_{ic} = \pm[\epsilon_\parallel/(|\eta|r_z)]\sqrt{1-(\delta z/r_z)^2}$, associated with the increasing local thermal spread. These spreads vary along bunch axis, ranging from all incoherent at mid-pulse ($\delta z = 0$), to all coherent at the bunch ends ($\delta z = \pm r_z$), and both coherent and incoherent in-between (plotted at 1/4 pulse, $\delta z/r_z = 1/2$). The compression is timed such that, shortly before full compression, the bunch is extracted from the ring into an extraction line for transport to the target. The RF voltages V are set for mid-pulse $(\Delta p/p)_{ic} = 1\%$ at full compression, corresponding to the chromatic focusing limit of the final focus optic. Since this envelope model is only consistent with linear focusing, the linear RF voltage V must be interpreted in terms of harmonic cavity superpositions (requiring additional RF voltage) sufficient to suppress nonlinear phase-space wrapping consistent with the prebunch extent in the phase of the fundamental RF harmonic[2].

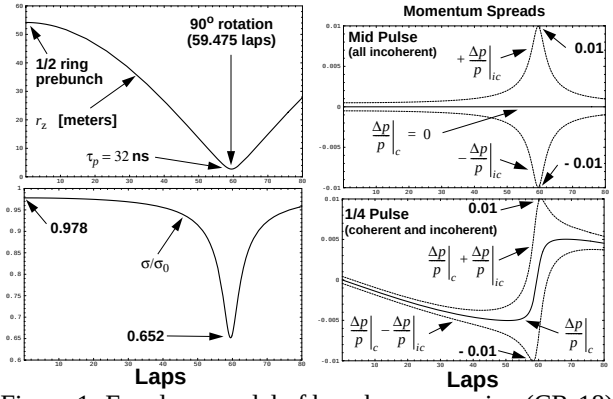

Figure 1: Envelope model of bunch compression (CR-18).

2.2 PIC Simulations

The combination of strong $\perp$ space-charge and large momentum spread in the ring/extraction line lead to issues in maintaining $\perp$ beam focusability (limiting emittance growth) that are being explored with 2d and 3d electrostatic PIC simulations based on the WARP code of LLNL[3] and several GSI codes. These simulations include lattices with varying levels of detail, a proper treatment of dispersion, and self-consistent space-charge fields. Presented here are $\perp$ 2d mid-pulse ($\delta z = 0$) simulations with a symmetric FODO lattice for $\perp$ focusing (occupancy of quadrupoles and dipoles are 25% and 15% of the lattice period, respectively, with tunes $Q_{x0} \simeq Q_{y0}$ equal to the mean of those in Table 1), and compression implemented by continuously adjusting the particle weights and momentum deviations consistent with the envelope model. The initial prebunch is modeled by loading an rms matched $\perp$ semi-Gaussian (uniform density and temperature) and a $\parallel$ Gaussian momentum spread (rms Neuffer equivalent) distributions and then advancing the coasting beam many laps to allow relaxation of the loaded distribution due to weak space-charge and dispersive effects in the ring. These mid-pulse simulations model the region of strongest space-charge and momentum spread, and are structured to explore physics issues as opposed to detailed design evaluations.

The rms emittance ($\epsilon_x = 4[\langle x^2\rangle\langle x'^2\rangle - \langle xx'\rangle^2]^{1/2}$, etc.) evolution is shown in Fig. 2 for a 180° phase-space rotation in the CR-18 lattice with zero (small N) and full current. At peak compression (90°, 59.475 laps), the in-bend-plane x-emittance undergoes a large increase, whereas the out-of-bend y-emittance undergoes a smaller, nonlinear space-charge driven increase. The thickness of the x-emittance trace indicates the amplitude of emittance oscillations at the lattice and betatron frequencies that result from dispersion and the distribution being dispersion mismatched due to the bunch compression, respectively. To better understand this, the x-particle equation of motion is well approximated by

$$x'' + \left(\frac{1}{\rho^2}\frac{1-\delta}{1+\delta} + \frac{\kappa_q}{1+\delta}\right)x = \frac{\delta}{1+\delta}\frac{1}{\rho} - \frac{q\partial\phi/\partial x}{m\gamma_s^2\beta_s^2c^2}, \quad (2)$$

where $\delta = \delta p/p$, ρ is the local bend radius, $\kappa_q = (\partial B_y/\partial x)/[B\rho]$ is the $\perp$ focusing strength of the magnetic quadrupoles, and ϕ is the self-field potential. Neglecting space-charge, chromatic effects [$\kappa_q/(1+\delta) \rightarrow \kappa_q$], and higher-order dispersive effects, $d\epsilon_x^2/ds = (32/\rho)[\langle x^2\rangle\langle x'\delta\rangle - \langle xx'\rangle\langle x\delta\rangle]$, showing that the emittance evolves primarily in the bends. For an uncorrelated initial distribution ($\langle x\delta\rangle = 0$, etc), it can be shown that $\epsilon_x^2(s) = \epsilon_x^2(0) + F(s)\epsilon_x(0)\langle\delta^2\rangle$, where $F(s)$ is a function (constant out of bends) depending only on the lattice. This oscillation can be understood by examining a group of particles with off-momentum δ. If the closed orbit of this particle group is shifted from the $\perp$ phase-space center of the group (from dispersion and dispersion mismatch), then the particles will betatron-rotate about the shifted orbit which oscillates according to the dispersion function. Hence, the phase-space ellipse bounding all off-momentum groups ($\sim \epsilon_x$) will oscillate with components at the betatron frequency (wavenumber k_β) and at the frequency of dispersion function oscillations ($2\pi/k \sim$ lattice period). The pumped momentum spread of the applied compression acts to increase the average and amplitude of the emittance oscillation. In this context, the emittance increase is a dispersion induced distortion that is reversible, and can be corrected in the extraction line with appropriate, compensating bends. However, this distortion influences the $\perp$ bunch size, and thereby the $\perp$ aperture and extraction. Moreover, nonlinear space-charge, chromatic, and higher-order dispersive effects can produce amplitude dependences that phase-mix (thermalize) part of these reversible emittance oscillations causing uncorrectable, "irreversible" growth.

Such growth must be limited, since it can also interfere with the correction of larger, reversible growth components. A measure of the irreversible growth is obtained in full 180° phase-space rotations, since these recover the initial momentum spread and emittance in the absence of irreversible effects. Small chromatic and dispersive terms prevent exact recovery in the zero current simulation shown. The emittance growth of these full-current simulations are qualitatively comparable with 180° rotation experiments[4].

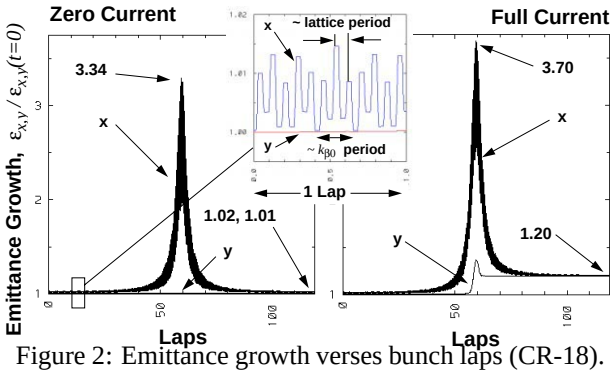

Figure 2: Emittance growth verses bunch laps (CR-18).

The dominant source of irreversible emittance growth appears to be nonlinear forces associated with space-charge modes launched during the compression. This is demonstrated by the simulations in Fig. 3, where the compression in Fig. 2 was carried out in a straight lattice ($\rho \to \infty$). Rapid growth occurs when σ/σ_0 becomes sufficiently depressed and remains when the compression is reversed. Negligible growth occurs for zero current, and space-charge instability induced growth can be reduced by adjusting $\perp$ focusing for $\sigma_0 < 90°$ to eliminate envelope and suppress higher-order collective modes. Little change was induced by varying the compression rate by factors of 2, suggesting fast instability saturation. Although these space charge instabilities are modified in a ring due to the $\perp$ dispersive broadening weakening space-charge forces, the $\sigma_0 < 90°$ criteria appears sufficient for rings. Reduced σ_0 also decreases envelope flutter, reducing sensitivity to focusing errors and problems associated with large envelope excursions combined with large momentum spread in bending dipoles. Unfortunately, this criteria is also inconsistent with long, low-dispersion straight sections (for bunch insertion/extraction, RF cavities, e^- cooling, etc.), since this requires high phase-advance through bends (with small superperiod number, M). However, in the presence of compression, strong space-charge, and large s-varying momentum spread, the conventional definition of a dispersion function D [$D = x/\delta$, where x is the closed orbit solution to Eq. (2) for δ small and $\phi \to 0$] carries little meaning. Large, s-varying space-charge strength and momentum spread in the compression result in a shift of D, complicating lattice design. From this perspective, the better approach appears to be a symmetric lattice with a large M ($\Rightarrow$ M = cell number), where the zero-current fluctuations of D are as small as possible. This minimizes reversible emittance growth at peak compression, reducing consequences of correction errors and irreversible growth.

Chromatic focusing effects and possibly other higher-order dispersive terms can phase-mix otherwise reversible distribution distortions into irreversible growth. Although these effects are typically weaker than space-charge induced nonlinearities, compensations should be considered. Also, since a momentum deviation δ is equivalent to all dipoles and quadrupoles having the same field error, tune values $Q_{x0} = Mk/2$ ($k = 1, 2, \cdots$) should be avoided. However, in a symmetric ring (M = cell number) the $\sigma_0 < 180°$ phase-advance limit for a valid $\perp$ bunch envelope preclude such resonances and likewise, low-order resonances due to systematic field errors. Resonances from construction errors are not regarded as troublesome due to the limited number of laps in the compression and detuning due to varying space-charge strength as the particles change $\parallel$ position in the bunch. This can be checked with full 3d simulations of distributions with realistic incoherent tune spreads. Finally, although results of 3d simulations with continuous, linear RF bunching differed little from the reduced 2d model presented, this must be re-evaluated for discrete RF cavities. The finite kick in δ provided by a discrete cavity leads to an instantaneous shift of the closed orbit of each group of off-momentum particles, which can lead to irreversible emittance growth when a series of kicks are applied. This can be properly evaluated in 3d simulations with realistic distributions of RF cavities.

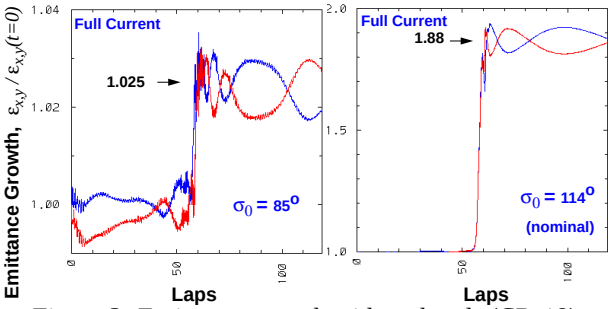

Figure 3: Emittance growth with no bends (CR-18).

3 CONCLUSIONS

This joint GSI/LLNL study is investigating the use of fast bunch rotation to compress a large number of particles in heavy-ion rings. The combination of large momentum spread and strong space charge in a ring creates challenges in limiting $\perp$ emittance growth. Simulations have distinguished and characterized reversible (correctable) growth due to dispersion induced distribution distortions and irreversible (uncorrectable) growth due to various effects. Tentative design criteria were developed to mitigate these growths. Tradeoffs between these constraints and practical considerations will be made in more optimal ring designs.

References

[1] P. Spiller, K. Blasche, O. Boine-Frankenheim, M. Emmerling, B. Franzcak, I. Hofmann, S. Lund, S. Lund, and U. Ratzinger, these proceedings.

[2] S. Lund, I. Hofmann, O. Boine-Frankenheim, and P. Spiller, to appear, GSI internal report (1999).

[3] D. Grote, Ph.D. Dissertation, Lawrence Livermore Laboratory, publication UCRL-LR-119363 (1994).

[4] R. Cappi, R. Garoby, D. Möhl, J.L. Vallet, and E. Wildner, in Proceeding of the 1994 European Particle Accelerator Conference, London, 27 June - 1 July, p. 279.